ELECTRONIC SUPPLEMENTARY INFORMATION

"*Trans*-Influence of Cyanide on the Structural and Electronic Properties of a Series of Organocobalt[III](TIM) Complexes"

Leobardo Rodriguez Segura and Tong Ren*

Department of Chemistry, Purdue University, West Lafayette, Indiana 47907, USA

*To whom correspondence should be addressed. Email: tren@purdue.edu

Table of Contents

Additional synthetic details

Synthesis of trans-[Co(TIM)(CN)$_2$]PF$_6$ (4). In a flask, [Co(TIM)Cl$_2$]PF$_6$ (502.5mg; 0.960 mmol) was dissolved in 30 mL of CH$_3$OH and 15 mL of CH$_3$CN. KCN (137.1 mg; 2.11 mmol) was added directly to the reaction flask. The reaction mixture rapidly turned a light orange color. After 5 min, the crude reaction was filtered through Celite using CH$_3$OH. Diethyl ether was added directly to the light orange-green filtrate until the solution became cloudy. After cooling at -15°C for 12 h, **4** was filtered out as a pale yellow-tan solid and washed with copious amounts of diethyl ether. Yield: 428.2 mg (0.849 mmol; 88%).

Synthesis of trans-[Co(TIM)(CH$_3$)I]PF$_6$ (5). Adapted from Ref.[1] In a 100 mL Schlenk flask, [Co(TIM)Cl$_2$]PF$_6$ (1.002 g; 1.92 mmol) was dissolved in 75 mL of a 4/1 acetone/CH$_3$OH mixture and purged with N$_2$. After 25 min, NaBH$_4$ (156.2 mg; 4.13 mmol) was added against a positive flow of N$_2$ causing the reaction mixture to turn a dark blue. Within a minute of obtaining the blue colored reaction, MeI (7 mL) was added resulting in an immediate color change to red-orange. After 5 min, the crude reaction mixture was filtered through Celite to remove excess and unreacted Na$^+$ salts—white and purple solid remained on the baseline. The red filtrate was collected and removed *in vacuo* with careful attention to avoid excess exposure to heat and ambient light. The remaining red-brown residue was taken up in CH$_2$Cl$_2$ and loaded onto a silica column plug. A 1/9 acetone/CH$_2$Cl$_2$ solvent mixture was used to elute a broad red-orange band. This was collected, and the solvent was removed. The remaining red-orange residue was taken up in MeCN and recrystallized via the addition of diethyl ether. Compound **5** precipitated out of solution as a red-orange solid. This was filtered out and dried under vacuum. Yield: 304.0 mg (0.051 mmol; 27% based on Co).

Synthesis of trans-[Co(TIM)(CH$_3$)$_2$]PF$_6$ (6). Adapted from Ref.[2] [Co(TIM)Cl$_2$]PF$_6$ (191.8 mg; 0.367 mmol) was dissolved in 30 mL of a 1/1 acetone/methanol mixture and heated to 50°C. The blue-green solution was filtered and returned to the reaction flask. Iodomethane (0.4 mL; 6.43 mmol) was added to the solution. In a separate beaker, NaBH$_4$ (38.1; 1.01 mmol) was dissolved in minimal water. The aq. NaBH$_4$ solution was added drop-wise to the blue-green reaction mixture, which instantly turned dark blue followed by dark red. After 5 min, NaPF$_6$ (48.0 mg; 0.286 mmol), dissolved in MeOH, was added to the reaction mixture. The solvent was reduced,

and red solid began to crash out. ESI-MS of the solid indicated the presence of **6** trace amounts of **5**. The solid was filtered out and the filtrate place in the freezer (-15°C). Red crystals of **6** suitable for x-ray diffraction studies were taken directly from the recrystallization flask.

Crystallographic details

Single Crystal X-ray Structure Analysis

Single crystals of **1**, **2**, and **4**–**6** were grown from slow diffusion of diethyl ether into a concentrated solution of the respective compounds in CH_3CN at -15°C. X-ray diffraction data for all crystals were obtained on a Bruker Quest diffractometer with a fixed chi angle, a sealed tube fine focus X-ray tube, a single crystal curved graphite incident beam monochromator, either a Photon II (**1**, **5**, and **6**) or Photon III (**2** and **4**) area detector, and an Oxford Cryosystems low temperature device. Data for **1**, **5**, and **6** were collected with Mo K_α radiation (λ=0.71073 Å) at 150K, and data for **2** and **4** were collected with Cu K_α radiation (λ=1.54178 Å) at 150K. Data were collected; reflections were indexed and processed using APEX4[3] and reduced using SAINT. The space groups were assigned and the structures were solved by direct methods using XPREP within the SHELXTL suite of programs,[4] solved using ShelXT,[5] and refined using Shelxl[6, 7] and Shelxle.[8]

If not specified H atoms attached to carbon atoms were positioned geometrically and constrained to ride on their parent atoms. C–H bond distances were constrained to 0.95 Å for aromatic and alkene C–H and CH_2 moieties, and to 0.99 and 0.98 Å for aliphatic CH_2 and CH_3 moieties, respectively. Methyl CH_3 hydroxyl H atoms were allowed to rotate but not to tip to best fit the experimental electron density. $U_{iso}(H)$ values were set to a multiple of $U_{eq}(C)$ with 1.5 for CH_3 and OH, and 1.2 for C–H, CH_2 and N–H units, respectively.

Crystallographic data for **1**, **2**, and **4**–**6** are provided below in Table S1. CCDC 2355970–2355974 contain the supplementary crystallographic data for compounds **1**, **2**, and **4**–**6**, respectively. These data can be obtained free of charge from The Cambridge Crystallographic Data Centre.

Table S1. Crystal data for complexes **1**, **2**, and **4**–**6**

	1	2	4	5	6
Chemical Formula	$C_{23}H_{31}CoN_5 \cdot F_6P$	$C_{27}H_{41}CoN_5 \cdot F_6P \cdot C_3H_6O$	$C_{16}H_{24}CoN_6 \cdot F_6P \cdot C_2H_3N$	$C_{15}H_{27}Cl_{0.08}Co I_{0.92}N_4 \cdot F_6P$	$C_{16}H_{30}CoN_4 \cdot F_6P$
Formula Weight	581.43	697.62	545.36	586.75	482.34
Space Group	Monoclinic, $P2_1/n$	Monoclinic, $P2_1/c$	Orthorhombic, $Pnma$	Tetragonal, $P\bar{4}2_1c$	Trigonal, $R\bar{3}{:}H$
a, Å	13.7682 (9)	10.6469 (2)	16.3877 (7)	15.4579 (7)	18.7533 (11)
b, Å	11.5417 (7)	22.5392 (5)	18.7783 (8)		-
c, Å	15.7248 (10)	14.0575 (3)	7.5802 (3)	17.5114 (15)	20.1833(11)
α, deg	-	-			-
β, deg	90.394 (3)	96.967 (1)			-
γ, deg	-	-			-
V, Å^3	2498.8 (3)	3348.51 (12)	2332.68 (17)	4184.3 (5)	6147.2 (8)
Z	4	4	4	8	12
T, K	150	150	150	150	150
λ, Å	0.71073	1.54178	1.54178	0.71073	0.71073
$\Delta\rho_{max}, \Delta\rho_{min}$ (e Å^{-3})	0.38, -0.57	0.57, -0.46	0.38, -0.42	0.67, -0.57	0.41, -0.37
R	0.036	0.041	0.032	0.026	0.046
$R_w(F^2)$	0.093	0.117	0.085	0.055	0.139

Special refinement details

Compound 1

One crystallographically independent anion site was found to be occupied by two unique hexafluorophosphate moieties. ADPs of the PF$_6$ atoms were restrained to have similar U_{ij} components (SIMU command of Shelxl) for atoms closer to each other than 2.0 Å. ESDs used were 0.01 Å^2. All bond lengths and angles were restrained to be the same for both moieties using a SAME command. Subject to these conditions the occupancy ratio refined to 0.836(6) to 0.164(6).

Compound 2

Within the macrocycle, one propylene bridge was found to be positioned above the plane of the ligand or below the plane. These were solved using a Part 1 and Part 2. ADPs of the carbon atoms were restrained to have U_{ij} components (SIMU command for Shelxl). ESDs were 0.01 Å^2. Subject to these conditions, the occupancy ratio refined to 0.898(5) to 0.102(5).

Compound 4

The hexafluorophosphate ion was found to occupy one of two positions wherein the F atoms rotated about the F2-P1-F3 axis. The two independent moieties were separated into Part 1 and Part 2. ADPs of the disordered atoms within 2.0 Å of each other were restrained to have similar U_{ij} components (SIMU command of Shelxl). ESDs were 0.01 Å^2. Subject to these conditions the occupancy ratio for the PF$_6$ anions refined to 0.910(3) to 0.090(3).

Compound 5

The structure was solved as being $P\bar{4}2_1c$ which allows for the possibility for inversion twinning. Refinement as a 2-component inversion twin resulted in a roughly 99:1 twin ratio (BASF value of 0.016(21)).

The hexafluorophosphate moiety centered on P3 is disordered around a two-fold axis and a mirror plane resulting in four symmetry equivalent PF$_6$ moieties upon placing all of the atoms in moiety in a Part -1. All PF$_6$ P-F bond distances were restrained to be similar to each other (SADI restraint of Shelxl). The bond angles in the P3 moiety were also restrained to be similar to each other using the SADI restraint to best model an octahedral geometry for the PF$_6$. ADPs of the PF$_6$ atoms around P3 were restrained to have similar U_{ij} components (SIMU command of Shelxl) for atoms closer to each other than 2.0 Å. ESDs used were 0.01 Å^2. The P3 atom was refined to behave approximately isotropic with an ESD of 0.001 Å^2.

Within the cation, the coordination site *trans* to the methyl ligand can be occupied by either an iodide or a chloride. The two possible halides were separated into Part 1 and Part 2. ADPs of the atoms were restrained to have identical U_{ij} components (EADP command of Shelxl). Subject to these conditions the occupancy ratio for the I:Cl anions refined to 0.921(2) to 0.079(2).

Compound 6

Four crystallographically independent moieties were present in the unit cell: one cation on an inversion center, one cation located on a three-fold rotation axis and an inversion center, one PF$_6$

anion being located on an inversion center and a three-fold rotation axis, and one PF_6 anion located on only an inversion center. The latter anion was also disordered.

The four moieties were divided into 4 residues: within the disordered moieties, all atoms closer to each other than 2.0 Å were restrained to have similar U_{ij} components using the SIMU command of Shelxl. ESDs used were 0.01 Å^2. In the Co(TIM) moiety found in RESI 2, one half of the ligand is symmetry independent, with the other half created by the inversion center. The ligand is also disordered by a three-fold axis, with the symmetry independent half molecule thus one third occupied. To overcome limitations of Shelxl (PART -1 either applying to both inversion and three-fold rotation, or to neither, preventing placement of H-atoms with AFIX commands and creating and incomplete bond and angle list), the symmetry equivalent by inversion of one of the nitrogen atoms (of N1_1) was added (N3_2), the two atoms were given each half occupancy (one sixth instead of one third), and the atoms were constrained to have exactly inversion related positions. The latter was accomplished by constraining the fractional atom coordinates along a, b and c to obey the inversion symmetry operation via constraining their sums to the values set by the symmetry operator, which was 2/3-x, 4/3-y, 1/3-z. The fractional coordinates along a for N1_1 and N3_3 were thus set to free variables, which were in turn constrained to add up to 2/3, along b to 4/3, and along c to 1/3:

> SUMP 0.66666666666666 0 1.0 4 1.0 7
> SUMP 1.33333333333333 0 1.0 5 1.0 8
> SUMP 0.33333333333333 0 1.0 6 1.0 9

.

The ADPs of N1_1 and N3_3 were also constrained to be identical: EADP_2 N1 N3. Once this was done, the one half of the ligand that is symmetry independent was restrained to have a similar geometry as its equivalent in the not disordered TIM ligand (RESI 1, SAME command) and H atoms were added using HFIX/AFIX commands as usual.

In RESI 4, the PF_6 anion occupied one of two positions. The disordered F atoms were divided into PART 1 and PART 2 with a free variable of 21.0000 and -21.0000. The P-F bond lengths and angles were restrained to be the same as those in the PF_6 anion found in RESI 3 using a SADI command. The occupancies refined to 0.350(24) to 0.650(24).
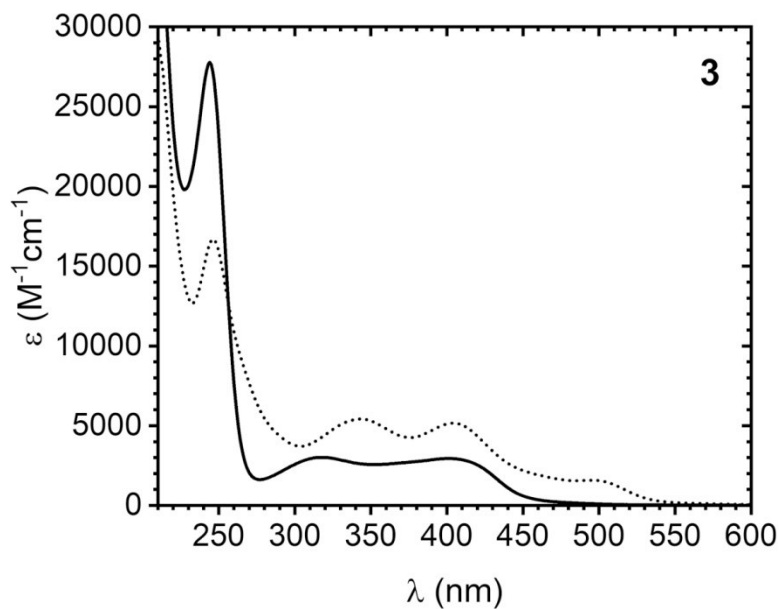
FTIR Spectra
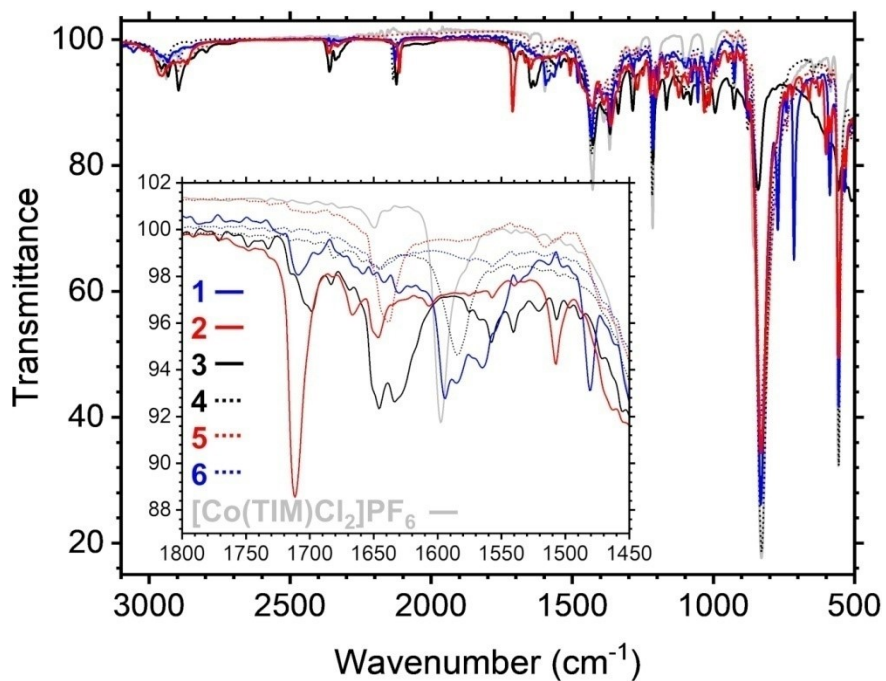
Fig. S1. FTIR spectra of **1–6** and *trans*-[Co(TIM)Cl$_2$]PF$_6$.

Absorbance Spectra
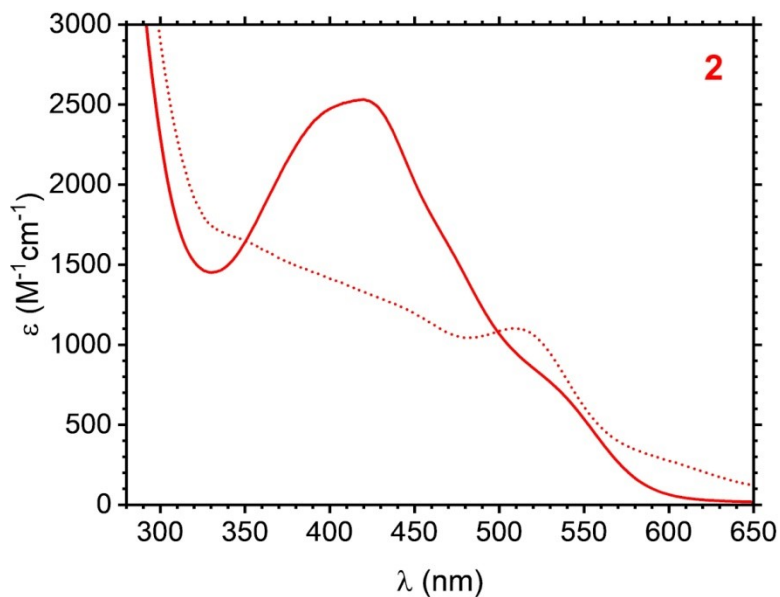
Fig. S2A. Absorbance spectra of **2** (solid trace) compared to [Co(TIM")(C(CH$_3$)C$_6$H$_4$-4-^{t}Bu)Cl]PF$_6$ (dotted trace) in CH$_3$CN.

Fig. S2B. Absorbance spectra of **3** (solid trace) compared to [Co(TIM)(CH$_3$)I]PF$_6$ (**5**, dotted trace) in CH$_3$CN.
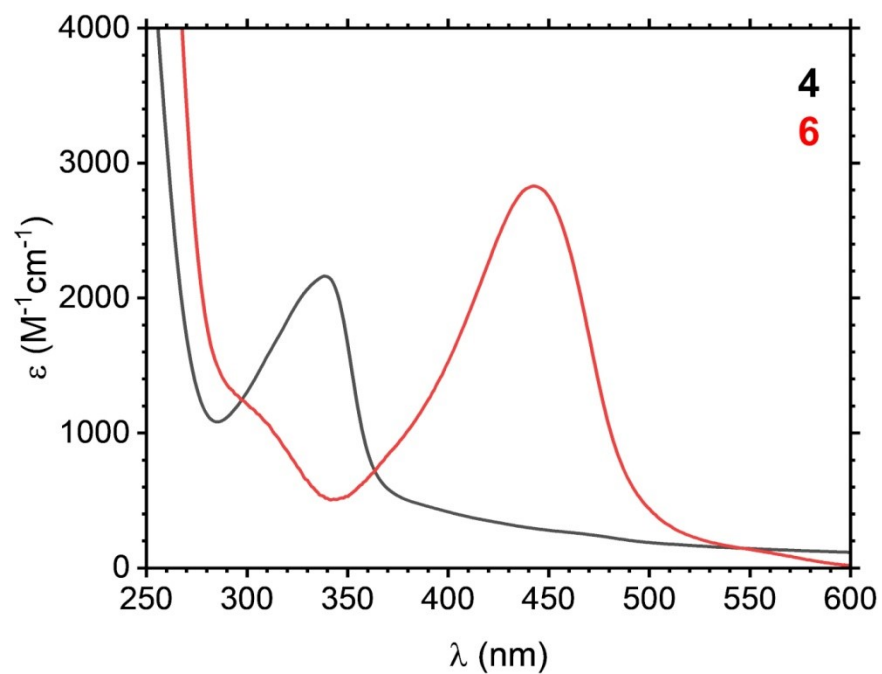

**Fig. S3.** Absorbance spectra of **4** and **6** in CH$_3$CN.

Electrochemical data

Additional Discussion: An emphasis on the seemingly limited impact of the *trans* influence of the cyanide on the oxidation potential of the *trans*-[Co(TIM)R(CN)]$^+$ (**1** and **3**) has been provided, especially in contrast to the effect on the same event in *trans*-[Co(TIM")R(CN)]$^+$ (**2**). However, cyanide is a strong σ-donor and does significantly increase the electron density at the Co^{III} center. As shown in Fig. S7, for the di-cyano complex, **4**, the Co-centered oxidation occurs at 0.67 V, which is considerably less positive than that in **1** (1.33 V); moreover, no oxidation events can be observed for [Co(TIM)Cl$_2$]$^+$ within the CH$_3$CN solvent window.[9]

Overall the highly irreversible nature of the Co-centered oxidation in **1**, **3**, and **5** is in contrast to previous electrochemical studies on monoalkylcobaloximes. In the latter complexes, electrochemical oxidations have been shown to proceed by a reversible 1 e$^-$ process to generate relatively stable alkycobalt(IV) species, which are predisposed to undergo nucleophilic displacement of the alkyl.[10, 11] It is probable that the *trans* anionic ligands in the Co(TIM) complexes lead to more labile alkycobalt^{IV}(TIM) species and result in faster displacement of the R groups. Notably, in **5** (Fig. S8) upon oxidation a cathodic event was observed during the return scan at -0.38 V, and repeated scans at positive potentials resulted in the deposition of an orange solid on the silver reference electrode for **5** but not for **1** and **3**. Nonetheless, the irreversibility of the Co$^{4+/3+}$ oxidation events in all three species is in agreement with previous studies of the di-methyl complex, **6**, for which Kochi and coworkers reported an irreversible electrochemical oxidation due to a follow-up chemical reaction.[12]
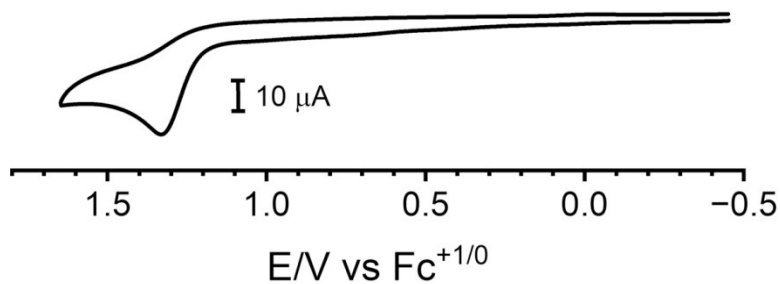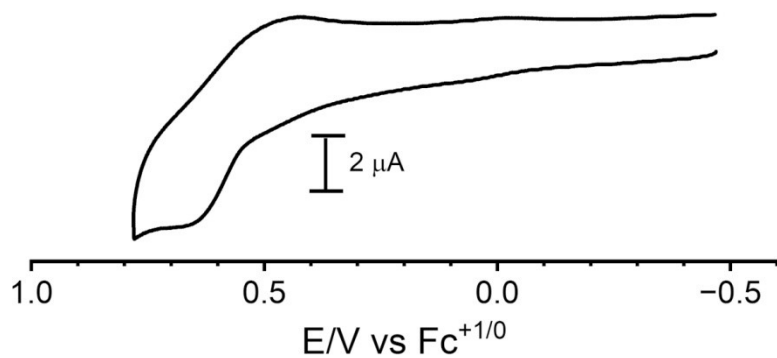
Fig. S4. Cyclic voltammogram of anodic scan of compound **1** (1.0 mM) recorded in 0.10 M CH$_3$CN solutions of [^{n}Bu$_4$N][PF$_6$] at a scan rate of 0.1 V/s.
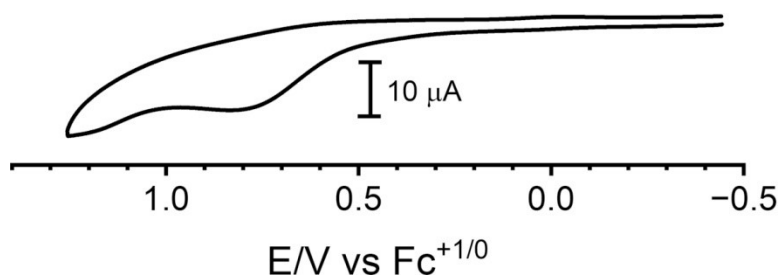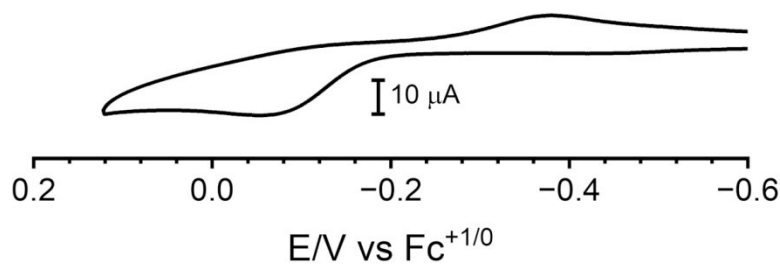

Fig. S5. Cyclic voltammogram of anodic scan of compound **2** (1.0 mM) recorded in 0.10 M CH$_3$CN solutions of [^{n}Bu$_4$N][PF$_6$] at a scan rate of 0.1 V/s.
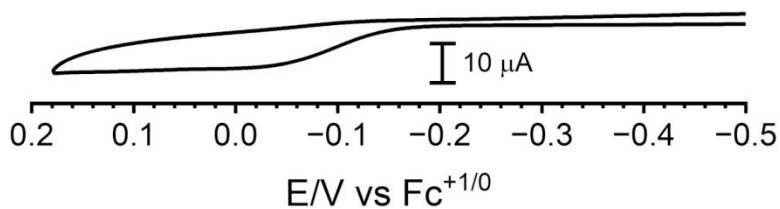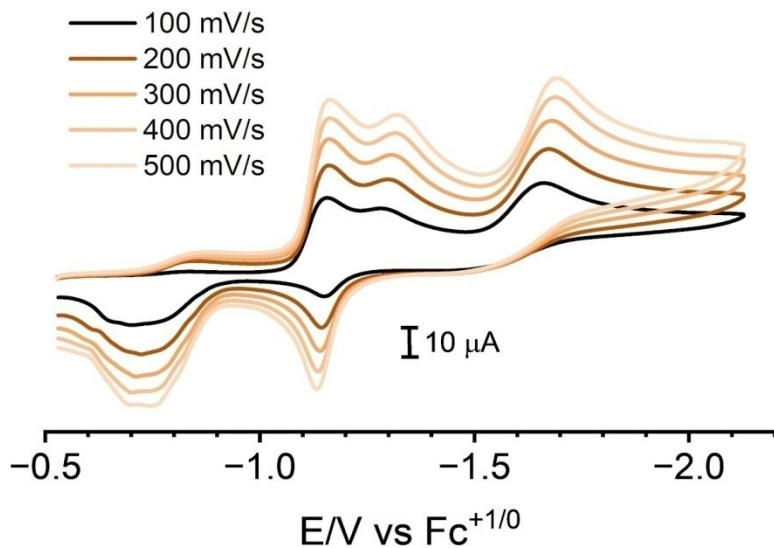

Fig. S6. Cyclic voltammogram of anodic scan of compound **3** (1.0 mM) recorded in 0.10 M CH$_3$CN solutions of [^{n}Bu$_4$N][PF$_6$] at a scan rate of 0.1 V/s.

Fig. S7. Cyclic voltammogram of anodic scan of compound **4** (1.0 mM) recorded in 0.10 M CH$_3$CN solutions of [^{n}Bu$_4$N][PF$_6$] at a scan rate of 0.1 V/s.
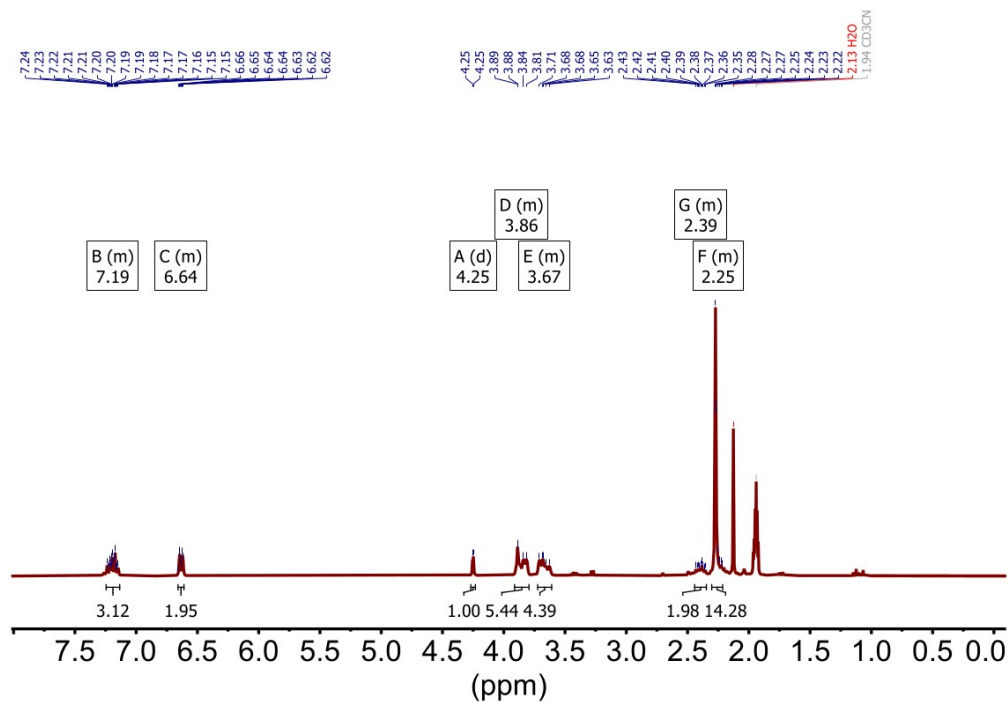

Fig. S8. Cyclic voltammogram of anodic scan of compound **5** (1.0 mM) recorded in 0.10 M CH$_3$CN solutions of [^{n}Bu$_4$N][PF$_6$] at a scan rate of 0.1 V/s.
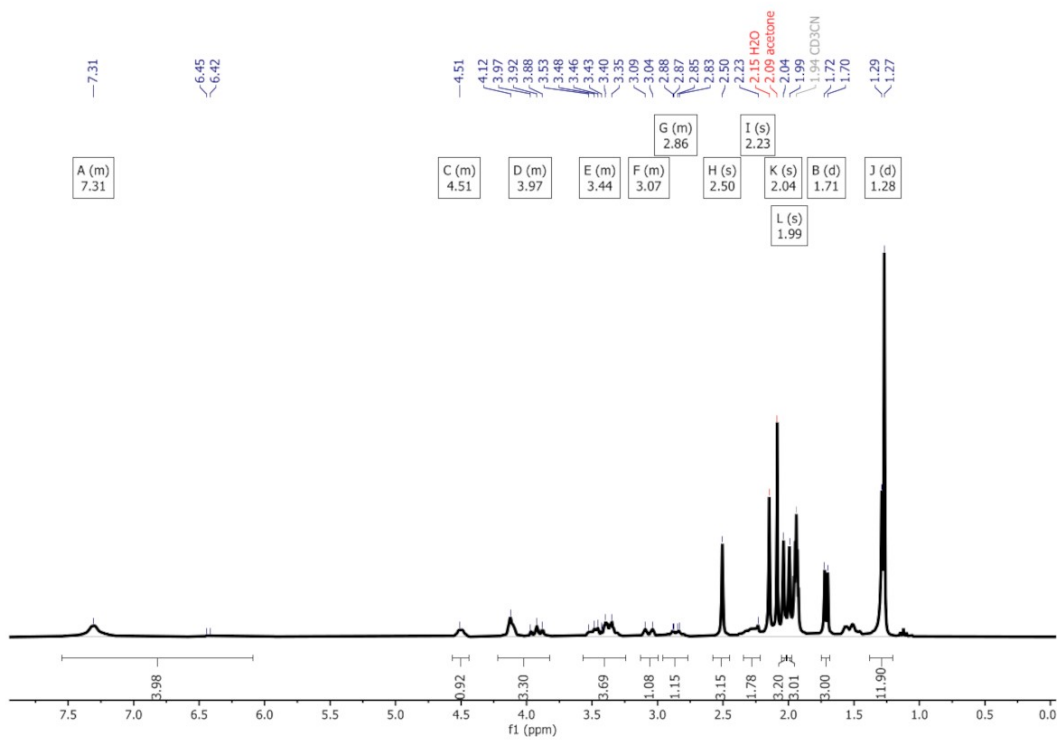

Fig. S9. Cyclic voltammogram of anodic scan of compound **5** (1.0 mM) recorded in 0.10 M CH$_3$CN solutions of [^{n}Bu$_4$N][PF$_6$] at varying scan rates.
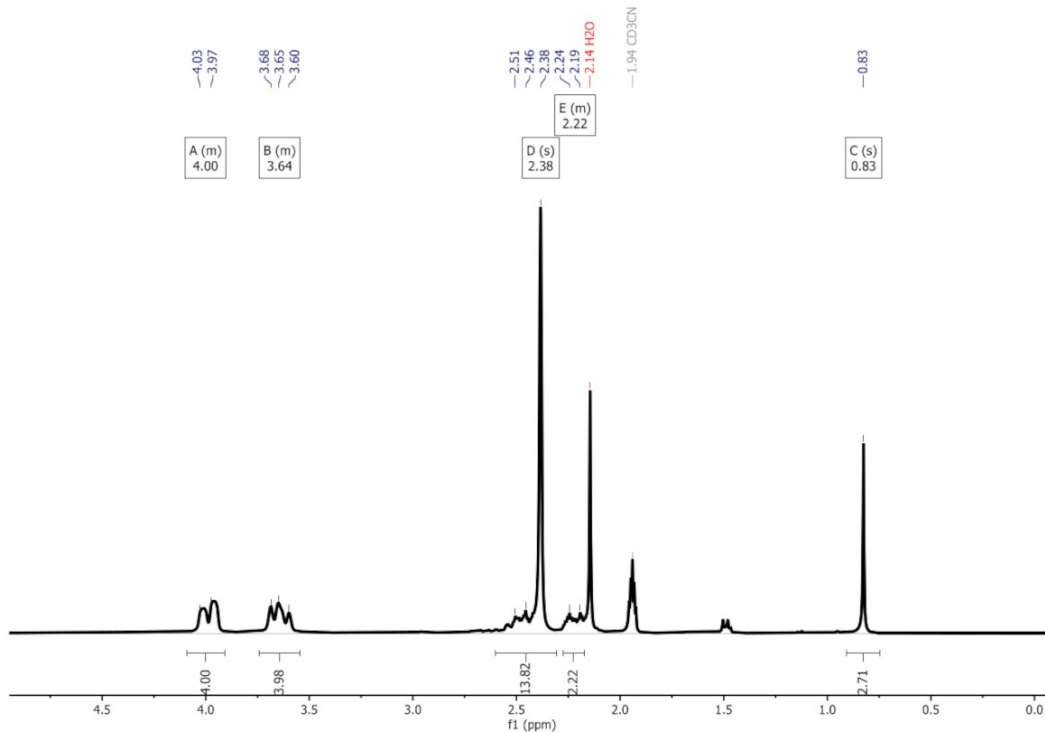
¹H NMR spectra

Fig. S10. ¹H NMR of [Co(TIM)(C(CH$_2$)Ph)(CN)]PF$_6$ (**1**) in CD$_3$CN.

Fig. S11. ¹H NMR of [Co(TIM'')(C(CH$_3$)C$_6$H$_4$-4-^{t}Bu)(CN)]PF$_6$ (**2**) in CD$_3$CN.

Fig. S12. ^{1}H NMR of [Co(TIM)(CH$_3$)(CN)]PF$_6$ (**3**) in CD$_3$CN.

References:

1   K. Farmery and D. H. Busch, *Inorg. Chem.*, 1972, **11**, 2901-2906.
2   S. Rapsomanikis, J. J. Ciejka and J. H. Weber, *Inorg. Chim. Acta.*, 1984, **89**, 179-183.
3   *APEX4 v2022.10-1, Saint V8.40B*, Bruker AXS, Inc.: Madison, WI, 2022.
4   *SHELXTL suite of programs, version 6.14*, 6.14; Bruker AXS Inc.: Madison, WI, 2000-2003.
5   G. M. Sheldrick, *Acta Cryst.*, 2015, A71 73--78.
6   G. M. Sheldrick, *Acta Crystallogr C*, 2015, **71**, 3-8.
7   G. M. Sheldrick *SHELXL2019*, Göttingen, Germany, 2019.
8   C. B. Hübschle, G. M. Sheldrick and B. Dittrich, *J. Appl. Cryst.*, 2011, **44**, 1281-1284.
9   L. Rodriguez Segura, S. A. Lee, B. L. Mash, A. J. Schuman and T. Ren, *Organometallics*, 2021, **40**, 3313-3322.
10   J. Halpern, M. S. Chan, J. Hanson, T. S. Roche and J. A. Topich, *J. Am. Chem. Soc.*, 1975, **97**, 1606-1608.
11   P. Abley, E. R. Dockal and J. Halpern, *J. Am. Chem. Soc.*, 1972, **94**, 659-660.
12   W. H. Tamblyn, R. J. Klingler, W. S. Hwang and J. K. Kochi, *J. Am. Chem. Soc.*, 1981, **103**, 3161-3172.